

Molecular Docking of Interaction between D7 Protein from the Salivary Gland of *Aedes aegypti* and Leukotriene A₄ for Developing Thrombolytic Agent

Syubbanul Wathon^{1*}, Rike Oktarianti¹, and Kartika Senjarini¹

¹Biology Department, Faculty of Mathematics and Natural Sciences, University of Jember, Jember, Indonesia

Abstract. The salivary glands of mosquitoes contain protein molecules that facilitate blood-feeding. One important protein in *Aedes aegypti* (*Ae. aegypti*) salivary glands is the D7 protein, which is known to inhibit platelet aggregation by binding to leukotriene A₄ molecules upon blood-feeding. Leukotriene A₄ is known as a molecule that improves platelet aggregation. This ability to bind to leukotriene A₄ demonstrates the potential of a new thrombolytic agent. This can be investigated through an in-silico study using the molecular docking method. The present study involved the 3D structure of the D7 protein and the Leukotriene A₄ ligand. It also comprised preparing their structures, validating the molecular docking method, and analyzing the outcomes. The result of the molecular docking documented an ΔG value of 6.63 kcal/mol, which signified stable and spontaneous binding between the D7 protein and the leukotriene A₄. The active site of the D7 protein when binding to the leukotriene A₄ ligand involves several amino acid residues, namely GLN 177, TYR 178, ARG 176, VAL 193, ILE 175, MET 194, PHE 154, PHE 186, HIS 189, TYR 248 and PHE 264. The ability to bind to leukotriene A₄, as an inducer of platelet aggregation, evidences the potential as a novel thrombolytic agent.

1 Introduction

Vectors have salivary glands which contain biological components associated with different functions [1]. These components serve as vasodilators and immunomodulatory factors influencing the host's immune response [2-3]. The vasodilator component is responsible for widening the host's blood vessels, eventually making it easier for mosquitoes to suck the host's blood. The immunomodulatory component modulates the host immune response [4]. Both of these components enable blood-feeding on the host. These components are also indirectly utilized by pathogens carried by vectors to penetrate the host's body [5]. For instance, the Dengue Hemorrhagic Fever (DHF) vector, *Ae. aegypti*, possesses salivary glands that are crucial in the blood-feeding process and transmitting the dengue virus into the human body [6].

* Corresponding author: syubbanulwathon@unej.ac.id

Components present in the salivary glands of *Ae. aegypti* commonly involves protein molecules required for the blood-feeding [7]. Proteins present in the salivary glands of *Ae. Aegypti* comprises Apyrase, Serpin, Adenosine Deaminase, the D7 family, and other proteins [8]. Apyrase is necessary in inhibiting platelet aggregation by hydrolyzing ATP and ADP into AMP [9-10]. Serpin is a protease inhibitor to serine protease activity in numerous hemostatic mechanisms in the host body [11]. As an anti-inflammatory component, adenosine deaminase inhibits the proteases secreted by mast cells [12]. D7 proteins are the most common components in the saliva of vectors, especially the *Aedes* genus [13].

D7 protein falls into a group of Odorant Binding Proteins in the salivary glands of vectors that affect the blood-feeding process to a host body [14]. D7 protein from the salivary glands of *Ae. aegypti* has also been known to be an immunogenic protein [15-16]. The protein can bind to biogenic amine and eucosanoid compounds generated by the host during blood-feeding [17]. One eucosanoid important in platelet aggregation is leukotriene A₄, which triggers thrombus formation in the wound area [18]. Leukotriene A₄ belongs to the eucosanoid group, a lipid-based chemical signal that affects cellular inflammatory response, vasoconstriction, and platelet aggregation [19]. Leukotriene A₄ stimulates platelet activation by binding to the leukotriene A₄ receptor on the platelet cell membrane [20]. D7 protein can bind to leukotriene A₄ as a eucosanoid component of the host during the blood-feeding process [21]. The bond between the D7 protein and leukotriene A₄ is reported to have antagonistic properties to the homeostasis of the host body. The bond can inhibit platelet aggregation in the wound area caused by the blood-feeding process [22]. The D7 protein from the salivary glands of *Ae. aegypti* inhibit platelet aggregation in the host body [23].

The ability of the D7 protein to inhibit platelet aggregation implies that it may afford the potential for a platelet anti-aggregation agent. The vectorial capacity of *Ae. aegypti*, known to be the key vector of DHF transmission, continues to be explored for biological components and functions in its salivary glands [24]. However, the ability of the D7 protein from *Ae. aegypti* salivary glands to bind to leukotriene A₄ is not fully understood. The present study aims to address this gap by exploring the interaction between D7 protein from *Ae. aegypti* salivary glands and leukotriene A₄ ligand. In-silico studies through molecular docking methods offer the advantage of predicting the interaction and binding mode of a target protein to a test ligand [25]. This method was undertaken to explore the protein's ability to bind to leukotriene A₄ which could be developed as a new candidate thrombolytic agent.

2 Materials and Methods

2.1 The Time and Site of the Study

The researchers conducted the study from April to August 2023 at the Biotechnology Laboratory of the Faculty of Mathematics and Sciences at the University of Jember.

2.2 Equipment and Materials

The study operationalized an ASUS laptop with Intel(R) Core™ i5-1035G1 (8 CPUs) processor specifications, ~1.2GHz with 8GB RAM. Furthermore, it employed AutoDock Tools 1.5.7 (Scripps Research Institute), Chem 3D 15.1 (Cambridge Soft), and BIOVIA Discovery Studio 2021. Some bioinformatics databases used are UniProt (<https://www.uniprot.org/>), SWISS-MODEL (<https://swissmodel.expasy.org/>), and also PubChem (<https://pubchem.ncbi.nlm.nih.gov/>).

2.3 Methods

2.3.1 Retrieving 3D Protein and Ligand

The amino acid sequence of the D7 protein from *Ae. aegypti* was retrieved from the UniProt database with accession number P18153. The 3D structure of the protein was derived from the D7 amino acid sequence of *Ae. aegypti*, which was obtained from the SWISS-MODEL database. The best quality 3D structure model of D7 protein was downloaded in .pdb file format [26]. The 3D structure model of the D7 protein used in this study with the STML code is 3dye.1 which has a native ligand L-Norepinephrine (LNR). The 3D structure of the Leukotriene A₄ ligand with accession number 5280383 was retrieved from the PubChem database in .sdf format [27].

2.3.2 Preparing and Optimizing the Structures of D7 Protein and LNR Native Ligand

With the aid of AutoDock Tools, the 3D structure of the protein binding to the native ligand was removed from any water molecules and non-functional ligands. Water molecules and other inessential residues were removed from the 3D structure. Afterwards, the 3D structure and the native ligand LNR were separated. Each 3D structure of the molecule was saved in distinctive .pdb files. The separated 3D structure of D7 protein was pretreated with AutoDock Tools, by adding polar hydrogen, checking Missing Atoms, and adding Kollman Charge. Charge equalisation and file settings were applied to the 3D structure by using the AutoDock4 program. The protein 3D structure was then saved in .pdbqt format [28]. The 3D structure of native ligand LNR was prepared by adding a Gasteiger charge and administering a non-polar merge. This enabled polar hydrogen to interact with the target protein residues [29]. The arrangement and selection of rotation points on the LNR native ligand through the torsion tree helped to determine the best rotation results in molecular docking. The prepared ligand structure was saved in .pdbqt format [28].

2.3.3 Validating Molecular Docking

Molecular docking was validated through the re-docking between the 3D structure of the D7 protein and that of the native ligand LNR. It aimed to examine the binding location between the D7 protein molecule and the test ligand leukotriene A₄ through gridding on a gridbox region. The re-docking was accomplished by using AutoDock Tools. Gridbox data, showing the position of ligand bound to the protein, included number point dimension (x, y, and z), spacing (Angstrom), and Gridbox centre (x, y, and z). The results were saved in a .txt file. This validation was performed through RMSD (Root Mean Square Deviation) lower than 2 Angstroms (< 2Å) [30].

2.3.4 Preparing 3D Structure of Leukotriene A4 Test Ligand

The 3D structure of the leukotriene A₄ ligand was prepared using Chem3D to maintain energy minimization. The energy minimization was carried out through the Force Field Molecular Mechanism (MM2) method. The structure of the leukotriene A₄ test ligand was saved in a .pdb file, which was further pretreated through AutoDock Tools. This pretreatment included the addition of polar hydrogen and Gasteiger charge and rotation settings, involving similar stages to those in the preparation of LNR native ligands. The preparation results were saved in a .pdbqt file.

2.3.5 Molecular Docking between D7 Protein and Leukotriene A₄ Test Ligand

The molecular docking between the 3D structure of the D7 protein and that of the test ligand leukotriene A₄ was done by using AutoDock Tools. The files containing a 3D structure of the protein and test ligand were pre-processed in .pdbqt format, and these files were put into one folder. AutoGrid4 and AutoDock4 programs were added subsequently. The D7 protein was set as the macromolecule, and the leukotriene A₄ test ligand was selected as the ligand for gridbox generation. The next phase was setting the gridbox by following the coordinates from the re-docking.

The results of the gridbox settings were saved in a.gpf file. The AutoGrid4 programme was run using the Command Prompt (CMD) command by following the previous gridbox settings. Parameter settings and protein recognition were done to enable the AutoDock4 program. The results were saved in a .dpf file. The AutoDock4 program was initiated using the Command Prompt command based on the Autogrid result and prior parameters [31].

2.3.6 Analyzing and Visualizing Molecular Docking Results between D7 Protein and Leukotriene A₄ Test Ligand

The molecular docking between the D7 protein and test ligand Leukotriene A₄ was analyzed to examine free energy value (ΔG), resultant bond, and amino acid residues involved in the eventual chemical bonds. The free energy value of molecular docking results between the D7 protein and leukotriene A₄ test ligand was compared with that from the molecular docking involving the D7 protein and native ligand LNR. This aimed at investigating the difference in free energy stemming from the bonds between molecules. BIOVIA Discovery Studio was operative to visualize the bonding between the 3D structure of the protein and the test ligand as well as the various amino acid residues [32].

3 Results and Discussion

3.1 The 3D Structure of D7 Protein from *Ae. aegypti*

The study examined the sequences of amino acid data retrieved from the D7 protein of *Ae. aegypti*. This data was obtained from the UniProt database with accession number P18153. The D7 protein data had an identity as 37 kDa salivary gland allergen Aed a 2. The D7 protein from *Ae. aegypti* was composed of 321 amino acid sequences. Table 1 shows the protein code and complete sequence of the D7 protein from *Ae. aegypti*.

Table 1. The amino acid sequence of the D7 protein from *Ae. aegypti*

Protein Data of D7 <i>Ae. aegypti</i> in <i>fasta</i> Format
>sp P18153 ALL2_AEDAE 37 kDa salivary gland allergen Aed a 2 OS=Aedes aegypti OX=7159 GN=D7 PE=1 SV=2 MKLPLLLAIVTTFSVVASTGPFDPPEMLFTFTRCMEDNLEDGPNRPLMLAKWKEWINEPVDSPATQC FGKCVLVR TGLYDPVAQKFDASVIQE QFKAYPSLGEKSKVEAYANAVQQLPSTNNDCAAVFKAYDPV HKAHKDTSKNLFHGNKELTKGLYEKLGKDIRQKKQSYFEFCENKYYPAGSDKRQQLCKIRQYTVLDD ALFKEHTDCVMKGI RYITKNNELDAEEV KRDFMQV N KDTKALEKVLNDCKSKEPSNAGEKSWHYKYC LVESVKKDDFKEAFDYREVR SQIYAFNL P K K Q V Y S K P A V Q S Q V M E I D G K Q C P Q

The modelling of protein 3D structure was performed with the aid of the homology modelling process in the SWISS-MODEL database. The process was based on D7 protein sequence data from *Ae. aegypti*. The 3D structure model of the D7 protein was selected with

STML ID code 3dye.1. The 3D structure was the D7 Protein Crystal Structure of the AED7-norepinephrine complex. A non-native ligand LNR was identified in the structure. The 3D structure of the D7 protein signified a monomer consisting of one protein chain (chain A). The 3D structure resulted from the visualization of the D7 protein structure using X-ray crystallography with a resolution of 1.75 Å. The resolution value of the 3D structure model was found to be satisfactory. The visualization of the protein structure showed the results of X-ray crystallography with a resolution value of < 2.5 Å, indicating that the structure visualization was more accurate [30]. Figure 1 below displays the 3D structure of the D7 3dye.1 protein.

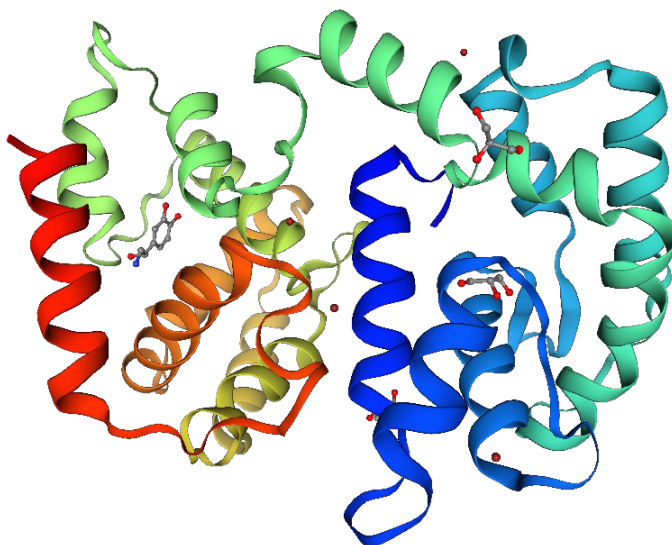


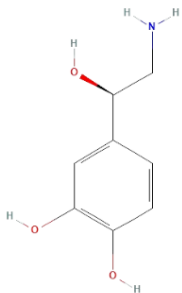
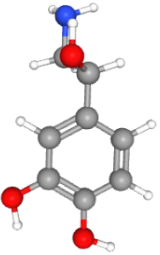
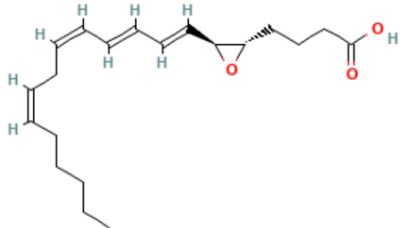
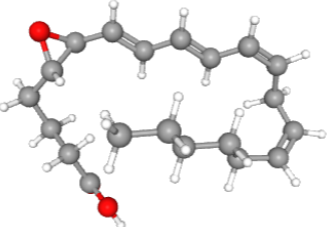
Fig. 1. 3D structure of D7 protein 3dye.1

3.2 The 3D Structure of Native Ligand LNR and Test Ligan Leukotriene A4

The native ligand in this study was derived from the 3D structure of the LNR ligand in the 3D structure model of D7 3dye.1 protein retrieved from the SWISS-MODEL database (Table 2). Native ligands were used to validate molecular docking and clarify the test ligands involved in the molecular docking. The LNR ligand has the molecular formula $C_8H_{11}NO_3$ [23].

The 3D structure of the human Leukotriene A4 ligand in this study was obtained from the PubChem database with accession number 5280383 (Table 2). Leukotriene played a role in platelet aggregation. Leukotrienes were involved in neutrophil recruitment, vascular leakage, and epithelial barrier function, while CysLTs induced bronchospasm and neutrophil extravasation, and were influential in vascular leakage of $C_{20}H_{30}O_3$ [33]. Leukotriene A4 molecule has the molecular formula $C_{20}H_{30}O_3$.

Table 2. The 2D dan 3D structures of LNR Ligand and Leukotriene A₄ Ligand

Ligand	Ligand Structure	
	2D	3D
L-Norepinephrine (LNR)		
Leukotriene A ₄		

3.3 Validating Molecular Docking Method

The target protein structure was prepared and optimized by removing water molecules and non-standard residues to accelerate the molecular docking [34]. Furthermore, the native ligand was separated from the target protein structure to create binding sites for the test ligand with the target protein throughout the molecular docking [35]. Therefore, the native ligand LNR was separated from the 3D structure of the D7 protein. Polar hydrogen atoms were added as the PDB 3D structure of the protein from X-ray crystallography might not possess hydrogen atoms, which would otherwise facilitate the bonding with the ligand [36]. The addition of hydrogen atoms helped to place or rotate hydrogen to stimulate the interactions between ligands and proteins [37]. Setting missing atoms aimed to check the missing atoms in the protein 3D structure because the PDB file may contain missing atoms [38]. The addition of Kollman Charge aimed to add electrostatic potential energy to the amino acids of the target protein [39].

Validation of the binding method began by setting the Gridbox coordinates for the re-docking between the target protein and native ligand. Setting the Gridbox coordinates was done by creating a space for the native ligand that would be bound to the target protein. The space obtained from the grid-box coordinates constituted an interaction site for the ligand and the target protein [40]. Gridbox settings were determined through coordinate points on the active side of the target protein, which included the coordinate values of grid size, grid centre, and grid spacing [41]. Gridbox coordinates settings in the re-docking process are displayed in Table 3. In the re-docking, the native ligand LNR formed a binding conformation with the 3D structure of the D7 protein of *Ae. aegypti* in the grid-box space.

Table 3. The setting of Gridbox coordinates in the 3D structure of protein from *Ae. aegypti*

<i>Grid Size</i>	<i>Grid Center</i>	<i>Grid Spacing</i>
x = 40	x = -0.612	0,375 Å
y = 40	y = 0.354	
z = 40	z = 29.11	

The molecular docking was examined to identify the RMSD value, which was obtained from the conformational alignment between the re-docking result of the native ligand and the conformation of the native ligand from crystallography. The smaller RMSD value indicates that the conformational position of the re-docking result ligand is close to the conformation of the original ligand position on the target protein. The RMSD value is considered valid when it is below 2 Å [36]. In this study, the validation documented an RMSD value of 1.130 Å. The overlap between the 3D structure of the native ligand LNR original conformation and the re-docking result conformation is shown in Figure 2. The re-docking result affirms satisfactory validation, the results of which can be used for further molecular docking between the 3D structures of the D7 protein and Leukotriene A₄ test ligand.

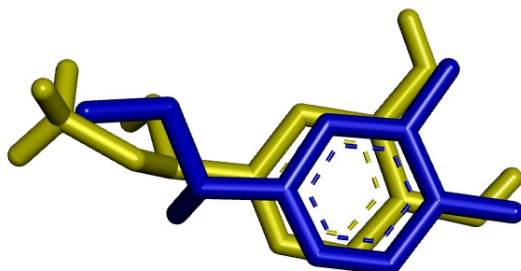


Fig. 2. The overlap between the 3D structure of the native ligand LNR original crystallographic conformation (blue) and the re-docking conformation (yellow)

3.4 Molecular Docking between 3D Structure of D7 protein from *Ae. aegypti* and Leukotriene A₄ Ligand

Leukotriene A₄ ligand preparation was done through energy minimization with MM2 settings to obtain a stable 3D conformation, which would enable the ligand to bind to the active side of the target protein [42]. The addition of hydrogen atoms aimed to bind the ligand to the target protein [37]. The non-polar merge setting allowed only polar hydrogen atoms to interact with the target protein residues [29]. Furthermore, ligand preparation through Compute Gasteiger Charges settings helped to add partial charges to the molecule [43].

Molecular docking was performed between the D7 protein and the prepared Leukotriene A₄ ligand. The molecular docking was performed using Gridbox settings from the re-docking results with the native ligand. The Gridbox coordinate settings were similar to those in the re-docking validation. This aimed to make the Leukotriene A₄ ligand bound to the active side region of the D7 protein. A rigid file setting was set on the D7 protein structure while a flexible setting was applied to the structure of the Leukotriene A₄ test ligand. The setting was aimed at forming a conformation by binding the test ligand to the active side of the target protein [44].

3.5 Analyzing and Visualizing Molecular Docking between D7 Protein and Leukotriene A₄ Ligand

The results of molecular docking between the test ligand and the target protein were evaluated through several parameters, including the types of bonds formed, the value of bond energy, and the amino acid residues on the active side of the target protein that interact with the ligand [45]. The Gibbs free energy (ΔG) or bond energy parameter corresponded to the amount of energy required to form a chemical bond on the active side of the D7 protein. The value of Gibbs free energy indicates the bond strength between the test ligand and the target protein [35].

The ΔG value of molecular docking results was found at -6.63 kcal/mol. This value indicates substantial energy released when a bond is formed between the ligand and the target protein. By contrast, a smaller ΔG value indicates less energy required to trigger the bond. This result indicates that the interaction between the protein and the ligand occurs spontaneously and in a stable state [46]. The ΔG value <0 indicates that the reaction is irreversible and spontaneous while $\Delta G = 0$ indicates a reversible reaction. The value of $\Delta G > 0$ indicates the absence of reaction [47]. The magnitude of negative ΔG indicates a stronger bond between the ligand and the target protein [48]. Negative ΔG indicates that the interaction between molecules occurs exothermically, meaning that the binding between the ligand on the active side of a protein is stable and spontaneous [49]. In the present study, the negative ΔG evinced that the D7 protein was able to bind to the Leukotriene A₄ molecule stably and spontaneously. In harmony with a previous study [23], this result corroborates that D7 protein from mosquito saliva can inhibit platelet aggregation during the blood-feeding process as it can bind and inhibit Leukotriene A₄.

The interaction between the D7 protein and Leukotriene A₄ ligand was explored with the aid of molecular docking. The visualization aided in the identification of the amino acid residues of a protein crucial in stimulating the interaction involving ligands [50]. Various amino acid residues on the active side of the target protein aid in forming interactions with ligands [29]. Several chemical bonds were created through the interactions between amino acids of a target protein and atoms on the test ligand, such as hydrogen bonds, alkyl interactions, pi-alkyl interactions, pi-sigma interactions, and pi-pi T-shaped interactions [51]. Figure 3 shows the results of molecular docking between the 3D structure of the D7 protein and the Leukotriene A₄ ligand.

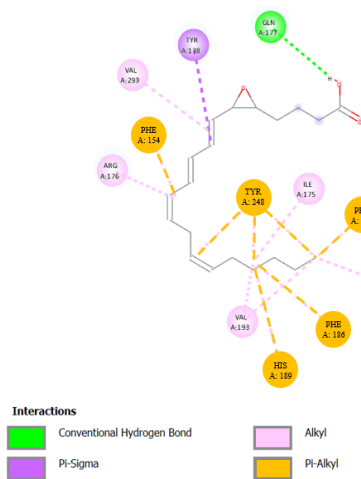


Fig 3. The interaction of amino acid residues of D7 protein with Leukotriene A₄ ligand

Table 4 describes the amino acid residues of the D7 protein interacting with Leukotriene A₄. The interaction indicates that the active side of D7 protein can bind to the Leukotriene A₄ ligand. The active side of D7 protein includes GLN 177, TYR 178, ARG 176, VAL 193, ILE 175, MET 194, PHE 154, PHE 186, HIS 189, TYR 248 and PHE 264. Chemical bonds resulting from these interactions involve conventional hydrogen bonds, Pi-Sigma bonds, alkyl interactions, and Pi-Alkyl interactions. Conventional hydrogen bonds are formed on one amino acid residue, GLN 177. Pi-Sigma bond is formed on one amino acid, TYR 178. Alkyl interactions are formed on four amino acid residues, inter alia, ARG 176, VAL 193, ILE 175, and MET 194. Pi-alkyl interaction is formed on five amino acids, among others, PHE 154, PHE 186, HIS 189, TYR 248, and PHE 264.

Table 4. The amino acid residues of D7 protein interacting with Leukotriene A₄

Amino Acid Residues	Atoms	Chemical Bonds
D7 Protein	Ligan Leukotriene A ₄	
Glutamine 177 (GLN 177)	H (Hydrogen)	Hydrogen bonds conventional
Tyrosine 178 (TYR 178)	C-H (Carbon Hydrogen)	Pi-Sigma bonds
Arginine 176 (ARG 176)	Alkyl	Alkyl
Valine 193 (VAL 193)	Alkyl	
Valine 193 (VAL 193)	Alkyl	
Valine 293 (VAL 293)	Alkyl	
Isoleucine (ILE 175)	Alkyl	
Metionine (MET 194)	Alkyl	Pi-Alkyl
Phenylalanine 154 (PHE 154)	Alkyl	
Phenylalanine 186 (PHE 186)	Alkyl	
Histidine 189 (HIS 189)	Alkyl	
Tyrosine 248 (TYR 248)	Alkyl	
Tyrosine 248 (TYR 248)	Alkyl	Pi-Alkyl
Tyrosine 248 (TYR 248)	Alkyl	
Phenylalanine 264 (PHE 264)	Alkyl	

Hydrogen bonds between proteins and ligands facilitate the binding to the active side [52]. The bonds occur between hydrogen atoms and electronegative atoms, such as fluorine (F), nitrogen (N), or oxygen (O) [53]. These bonds consist of conventional hydrogen bonds and carbon-hydrogen bonds. Conventional hydrogen bonding occurs because the donor and acceptor atoms have strong electronegativity [54]. Hydrogen bonds affect the stability of protein structure. This happens because proteins are formed from NH and OH groups that act as electron donors in forming hydrogen bonds, and electrons will be accepted by other groups [55]. Pi-Sigma bonds occur between Pi bonds and sigma bonds. Pi bonds tend to be weaker than sigma bonds because hybridization in pi bonds occurs laterally, with side-by-side hybrid orbitals and no paired electrons in one orbit. This causes the electrons to interact more easily with other, more electropositive atoms. As a result, pi bonds break more easily than sigma bonds [56].

Alkyl bonds occur in alkyl groups, which are defined as non-pi and non-polarised systems whose side chains are mostly aliphatic amino acids. These amino acids include alanine, valine, leucine, isoleucine, methionine, selenomethionine, cysteine, proline, CB, CG, and CD atoms of lysine, and CB and CG atoms of arginine. Alkyl denotes an organic chemical group containing only carbon and hydrogen atoms, constituting a chain. Pi-alkyl interactions occur in the pi electron cloud with an aromatic group and electron groups of several alkyl groups. Pi-alkyl interactions occur when the centroid of the pi ring and the alkyl group are inside the alkyl centroid and have at least a pair of nearest atoms with similar pi-pi [57].

4 Conclusion

The outcomes of molecular docking between D7 protein from *Ae. aegypti* to Leukotriene A₄ ligand have demonstrated a binding energy value of -6.63 kcal/mol. This has confirmed that D7 protein can stably and spontaneously bind to Leukotriene A₄. Amino acid residues on the active side of D7 protein that interact with atoms on the Leukotriene A₄ include GLN 177, TYR 178, ARG 176, VAL 193, ILE 175, MET 194, PHE 154, PHE 186, HIS 189, TYR 248 and PHE 264. The interactions between D7 protein residues and Leukotriene A₄ ligand comprise conventional hydrogen bonds, Pi-Sigma bonds, alkyl interactions, and Pi-Alkyl interactions. The findings acknowledge the potential of the D7 protein from *Ae. aegypti* as a new thrombolytic agent for the advancement in health and pharmaceutical fields.

References

1. D. Guerrero, T. Cantaert, D. Missé, Aedes Mosquito Salivary Components and Their Effect on the Immune Response to Arboviruses. *Front Cell Infect Microbiol.* 10 (2020).
2. S. Wathon, W. Purwati, R. Oktarianti, K. Senjarini, IgG Immune Response Against Salivary Gland Protein Extract of Dengue Vector *Aedes aegypti*, *JABS.* 16, 3 (2022).
3. R. Oktarianti, D. R. Damara, S.-R. Qudsiyah, S. Wathon, K. Senjarini, In vitro analysis of human immune response (IgG) against salivary gland extract of dengue vector from dengue hemorrhagic fever (DHF) endemic area in Jember, Indonesia. *IOP Conf. Ser.: Earth Environ. Sci.* 913, 012090 (2021). <https://doi.org/10.1088/1755-1315/913/1/012090>
4. J.-S. Clinton, M. B. Vogt, A. R. Kneubehl, B. M. Hibl, S. Paust, R. Rico-Hesse, Sialokinin in mosquito saliva shifts human immune responses towards intracellular pathogens. *PLoS Negl Trop Dis.* 17, e0011095 (2023). <https://doi.org/10.1371/journal.pntd.0011095>
5. A. Marín-López, H. Raduwan, T.-Y. Chen, S. Utrilla-Trigo, D.-P. Wolfhard, E. Fikrig, Mosquito Salivary Proteins and Arbovirus Infection: From Viral Enhancers to Potential Targets for Vaccines. *Pathogens.* 12, 3 (2023). <https://doi.org/10.3390/pathogens12030371>
6. O. López-Cuevas, J.-P. González-Gómez, J.-R. Aguirre-Sánchez, B. Gomez-Gil, E.-H. Torres-Montoya, J.-A. Medrano-Félix, C.-I. Martínez-Rodríguez, N. Castro-del Campo, C. Chaidez, Genomic Characterization of Twelve Lytic Bacteriophages Infecting Midgut Bacteria of *Aedes aegypti*. *Curr Microbiol* 79, 385 (2022). <https://doi.org/10.1007/s00284-022-03092-0>
7. Aisyah, R. Oktarianti, K. Senjarini, S. Wathon, Humoral Immune Response (IgG) of BALB/c Mice (*Mus musculus*) Post-injection by 56 kDa Immunogenic Protein Extract from the Salivary Glands of *Aedes aegypti* L. 4th International Conference on Life

- Sciences and Biotechnology (ICOLIB 2021), Atlantis Press. 157–167 (2022). https://doi.org/10.2991/978-94-6463-062-6_16
8. S. Wichit, P. Ferraris, V. Choumet, D. Missé, The effects of mosquito saliva on dengue virus infectivity in humans. *Curr Opin Virol.* 21, 139–145 (2016). <https://doi.org/10.1016/j.coviro.2016.10.001>
 9. A. Chowdhury, C.-M. Modahl, D. Missé, R.-M. Kini, J. Pompon, High resolution proteomics of *Aedes aegypti* salivary glands infected with either dengue, Zika or chikungunya viruses identify new virus specific and broad antiviral factors. *Sci Rep.* 11, 23696 (2021). <https://doi.org/10.1038/s41598-021-03211-0>
 10. R. Oktarianti, A. Suhardiansyah, E. Erni, S. Wathon, K. Senjarini, The Apyrase Functional Properties of the 56 kDa Protein from *Aedes aegypti* Salivary Gland. 4th International Conference on Life Sciences and Biotechnology (ICOLIB 2021), Atlantis Press. 135–143 (2022). https://doi.org/10.2991/978-94-6463-062-6_14
 11. G. Shrivastava, P.-C. Valenzuela-Leon, A.-C. Chagas, O. Kern, K. Botello, Y. Zhang, I. Martin-Martin, M.-B. Oliveira, L. Tirloni, E. Calvo, Albosepin, the Main Salivary Anticoagulant from the Disease Vector *Aedes albopictus*, Displays Anti-FXa-PAR Signaling In Vitro and In Vivo. *ImmunoHorizons.* 6, 373–383 (2022). <https://doi.org/10.4049/immunohorizons.2200045>
 12. Z. Li, C. Ji, J. Cheng, M. Åbrink, T. Shen, X. Kuang, Z. Shang, J. Wu, *Aedes albopictus* salivary proteins adenosine deaminase and 34k2 interact with human mast cell specific proteases tryptase and chymase. *Bioengineered* 13, 13752–13766 (2022). <https://doi.org/10.1080/21655979.2022.2081652>
 13. M.-J. Conway, B. Londono-Renteria, A. Troupin, A. M. Watson, W.-B. Klimstra, E. Fikrig, T.-M. Colpitts, *Aedes aegypti* D7 Saliva Protein Inhibits Dengue Virus Infection. *PLoS Negl Trop Dis.* 10, e0004941 (2016). <https://doi.org/10.1371/journal.pntd.0004941>
 14. P.-H. Alvarenga, P.-H. Alvarenga, D.-R. Dias, X. Xu, I.-M. Francischetti, A.-G. Gittis, G. Arp, D.-N. Garboczi, J.-M. Ribeiro, J.-F. Andersen, Functional aspects of evolution in a cluster of salivary protein genes from mosquitoes. *Insect Biochem. Mol. Biol.* 146, 103785 (2022). <https://doi.org/10.1016/j.ibmb.2022.103785>
 15. K. Senjarini, S. Atmandaru, A.-S. Nugraha, S. Wathon, R. Oktarianti, In Silico Study of Antigenicity and Immunogenicity of the D7 Protein from Salivary Glands of *Aedes aegypti*. 4th International Conference on Life Sciences and Biotechnology (ICOLIB 2021), Atlantis Press. 588–595 (2022). https://doi.org/10.2991/978-94-6463-062-6_60
 16. I. Zakiyyah, L.-D. Santika, S. Wathon, K. Senjarini, R. Oktarianti, Electroelution of 31 kDa Immunogenic Protein Fraction from the Salivary Gland of *Aedes aegypti* and *Aedes albopictus* (Diptera: Culicidae). 4th International Conference on Life Sciences and Biotechnology (ICOLIB 2021), Atlantis Press. 234–248 (2022). https://doi.org/10.2991/978-94-6463-062-6_23
 17. W. Jablonka, I.-H. Kim, P.-H. Alvarenga, J.-G. Valenzuela, J.-C. Ribeiro, J.-F. Andersen, Functional and structural similarities of D7 proteins in the independently-evolved salivary secretions of sand flies and mosquitoes. *Sci Rep.* 9, 1 (2019). <https://doi.org/10.1038/s41598-019-41848-0>
 18. P.-H. Alvarenga, J.-F. Andersen, An Overview of D7 Protein Structure and Physiological Roles in Blood-Feeding Nematocera. *Biology* 12, 1. (2023). <https://doi.org/10.3390/biology12010039>

19. M. Szczuko, I. Koziół, D. Kotłęga, J. Brodowski, A. Drozd, The Role of Thromboxane in the Course and Treatment of Ischemic Stroke: Review. *Int J Mol Sci.* 22, 21 (2021). <https://doi.org/10.3390/ijms222111644>
20. Q. Xiang, X. Pang, Z. Liu, G. Yang, W. Tao, Q. Pei, Y. Cui, Progress in the development of antiplatelet agents: Focus on the targeted molecular pathway from bench to clinic. *Pharmacol. Ther.* 203, 107393 (2019). <https://doi.org/10.1016/j.pharmthera.2019.107393>
21. I. Martin-Martin, O. Kern, S. Brooks, L.-B. Smith, P.-C. Valenzuela-Leon, B. Bonilla, H. Ackerman, E. Calvo, Biochemical characterization of AeD7L2 and its physiological relevance in blood feeding in the dengue mosquito vector, *Aedes aegypti*. *The FEBS Journal.* 288, 2014–2029, (2021). <https://doi.org/10.1111/febs.15524>
22. A. Fontaine, I. Diouf, N. Bakkali, D. Missé, F. Pagès, T. Fusai, C. Rogier, L. Almeras, Implication of haematophagous arthropod salivary proteins in host-vector interactions. *Parasites Vectors.* 4, 187 (2011). <https://doi.org/10.1186/1756-3305-4-187>
23. I. Martin-Martin, L.-B. Smith, A.-C. Chagas, A. Sá-Nunes, G. Shrivastava, P.-C. Valenzuela-Leon, E. Calvo, *Aedes albopictus* D7 Salivary Protein Prevents Host Hemostasis and Inflammation. *Biomolecules.* 10, 10 (2020). <https://doi.org/10.3390/biom10101372>
24. V.-H. Ferreira-de-Lima, P.-S. Andrade, L. M. Thomazelli, M. T. Marrelli, P.-R. Urbinatti, R.-S. Almeida, T.-N. Lima-Camara, Silent circulation of dengue virus in *Aedes albopictus* (Diptera: Culicidae) resulting from natural vertical transmission. *Sci Rep.* 10, 3855 (2020). <https://doi.org/10.1038/s41598-020-60870-1>
25. P.-M. Torres, A.-R. Sodero, P. Jofily, F.-P. Silva-Jr, Key Topics in Molecular Docking for Drug Design. *Int. J. Mol. Sci.* 20, 18 (2019). <https://doi.org/10.3390/ijms20184574>
26. S. Bienert, A. Waterhouse, T.-A. De Beer, G. Tauriello, G. Studer, L. Bordoli, T. Schwede, The SWISS-MODEL Repository—new features and functionality. *Nucleic Acids Res.* 45, D313–D319 (2017). <https://doi.org/10.1093/nar/gkw1132>
27. Y. Wang, S.-H. Bryant, T. Cheng, J. Wang, A. Gindulyte, B.-A. Shoemaker, P.-A. Thiessen, S. He, J. Zhang, PubChem BioAssay: 2017 update. *Nucleic Acids Res.* 45, D955–D963 (2017). <https://doi.org/10.1093/nar/gkw1118>
28. W.-R. Huey, G.-M. Morris, S. Forli, Using AutoDock 4 and AutoDock Vina with AutoDockTools: A Tutorial. (The Scripps Research Institute Molecular Graphics Laboratory, 2012).
29. I.-W. Sari, J. Junaidin, D. Pratiwi, Studi Molecular Docking Senyawa Flavonoid Herba Kumis Kucing (*Orthosiphon stamineus* B.) Pada Reseptor A-Glukosidase Sebagai Antidiabetes Tipe 2. *FARM.* 7, 54 (2020).
30. D. Ramírez J. Caballero, Is It Reliable to Take the Molecular Docking Top Scoring Position as the Best Solution without Considering Available Structural Data? *Molecules.* 23, 5 (2018). <https://doi.org/10.3390/molecules23051038>
31. N.-C. Endriyatno M. Walid, Studi In Silico Kandungan Senyawa Daun Srikaya (*Annona squamosa* L.) terhadap Protein Dihydrofolate Reductase pada *Mycobacterium tuberculosis*. *Pharmacon.* 19, 1 (2022). <https://doi.org/10.23917/pharmacon.v19i1.18044>
32. D.-N. Minovski, Molecular Docking Calculations Utilizing Discovery Studio & Pipeline Pilot. Laboratory for Cheminformatics (National Institute of Chemistry, Ljubljana, Slovenia, 2021).

33. A. Jo-Watanabe, T. Okuno, T. Yokomizo, The Role of Leukotrienes as Potential Therapeutic Targets in Allergic Disorders. *Int. J. Mol. Sci.* 20, 14 (2019). <https://doi.org/10.3390/ijms20143580>
34. S.-A. Attique, M. Hassan, M. Usman, R.-M. Atif, S. Mahboob, K.-A. Al-Ghanim, M.-M.-Z. Bilal, Nawaz, A Molecular Docking Approach to Evaluate the Pharmacological Properties of Natural and Synthetic Treatment Candidates for Use against Hypertension. *Int. J. Environ. Res. Public Health.* 16, 6 (2019). <https://doi.org/10.3390/ijerph16060923>
35. N.-P. Susanti, N.-L. Laksyani, N.-M. Noviyanti, K.-M. Arianti, I.-K. Duantara, Molecular Docking Terpinen-4-Ol Sebagai Antiinflamasi Pada Aterosklerosis Secara In Silico. *JCHEM.* 221 (2019). <https://doi.org/10.24843/JCHEM.2019.v13.i02.p16>
36. L. Ferencz D. L. Muntean, Identification of new superwarfarin-type rodenticides by structural similarity. The docking of ligands on the vitamin K epoxide reductase enzyme's active site. *Acta Univ. Sapientiae, Agric. Environ.* 7, 108–122 (2015).
37. G. Madhavi Sastry, M. Adzhigirey, T. Day, R. Annabhimoju, W. Sherman, Protein and ligand preparation: parameters, protocols, and influence on virtual screening enrichments. *J Comput Aided Mol Des.* 27, 221–234 (2013). <https://doi.org/10.1007/s10822-013-9644-8>
38. G. Duan, C. Ji, and J.-H. Zhang, Developing an effective polarizable bond method for small molecules with application to optimized molecular docking. *RSC Advances* 10, 15530–15540 (2020). <https://doi.org/10.1039/D0RA01483D>
39. J. Kolina, S. Sumiwi, J. Levita, Mode Ikatan Metabolit Sekunder di Tanaman Akar Kuning (*Arcangelisia Flava* L.) dengan Nitrat Oksida Sintase. *FITOFARMAKA* 8, 45–52 (2019). <https://doi.org/10.33751/jf.v8i1.1171>
40. M.-I. Alhazmi, Molecular docking of selected phytochemicals with H1N1 Proteins. *Bioinformation*, 11, 196–202 (2015). <https://doi.org/10.6026/97320630011196>
41. D. Afriza, W.-H. Suriyah, S.-A. Ichwan, In silico analysis of molecular interactions between the anti-apoptotic protein survivin and dentatin, nordentatin, and quercetin. *J. Phys.: Conf. Ser.* 1073, 032001 (2018). <https://doi.org/10.1088/1742-6596/1073/3/032001>
42. A. Fadlan Y. R. Nusantoro, The Effect of Energy Minimization on The Molecular Docking of Acetone-Based Oxindole Derivatives. *JKPK.* 6, 1 (2021). <https://doi.org/10.20961/jkpk.v6i1.45467>
43. M.-A. Alsafi, D.-L. Hughes, M.-A. Said, First COVID-19 molecular docking with a chalcone-based compound: synthesis, single-crystal structure and Hirshfeld surface analysis study. *Acta Cryst C.* 76, 1043–1050 (2020). <https://doi.org/10.1107/S2053229620014217>
44. L. Martínez, Automatic Identification of Mobile and Rigid Substructures in Molecular Dynamics Simulations and Fractional Structural Fluctuation Analysis. *PLoS One.* 10, e0119264 (2015). <https://doi.org/10.1371/journal.pone.0119264>
45. M.-F. Pratama, Studi Docking Molekular Senyawa Turunan Kuinolin Terhadap Reseptor Estrogen-A: Study of Molecular Docking of Quinoline Derivative Compounds against Estrogen-A Receptors. *Jurnal Surya Medika (JSM).* 2, 1 (2016). <https://doi.org/10.33084/jsm.v2i1.215>
46. A. Arwansyah, L. Ambarsari, T. Sumaryada, Simulasi Docking Senyawa Kurkumin dan Analognya Sebagai Inhibitor Reseptor Androgen pada Kanker Prostat. *Current Biochemistry.* 1, 11–19 (2014). <https://doi.org/10.29244/cb.1.1.11-19>

47. C. Wang, X. Cao, M. Dong, L. Zhang, J. Liu, X. Cao, X. Xue, Theoretical Calculation of Self-Propagating High-Temperature Synthesis (SHS) Preparation of AlB₁₂. ChemRxiv. (2021). <https://doi.org/10.26434/chemrxiv.13591427.v1>
48. M. Umamaheswari, A. Madeswaran, K. Asokkumar, Virtual Screening Analysis and In-vitro Xanthine Oxidase Inhibitory Activity of Some Commercially Available Flavonoids. Iran J Pharm Res. 12, 317–323 (2013).
49. N. Forouzesah, N. Mishra, An Effective MM/GBSA Protocol for Absolute Binding Free Energy Calculations: A Case Study on SARS-CoV-2 Spike Protein and the Human ACE2 Receptor. Molecules. 26, 8 (2021). <https://doi.org/10.3390/molecules26082383>
50. K. Furmanová, B. Kozlíková, V. Vonásek, J. Byška, DockVis: Visual Analysis of Molecular Docking Data. Eurographics Workshop on Visual Computing for Biology and Medicine. 10 (2019). <https://doi.org/10.2312/VCBM.20191238>
51. D. Kumar, R. Kumar, R. Ramajayam, K.-W. Lee, D.-S. Shin, Synthesis, Antioxidant and Molecular Docking Studies of (-)-Catechin Derivatives. J. Korean Chem. Soc. 65, 106–112 (2021). <https://doi.org/10.5012/jkcs.2021.65.2.106>
52. R. Kataria, A. Khatkar, In-silico design, synthesis, ADMET studies and biological evaluation of novel derivatives of Chlorogenic acid against Urease protein and H. Pylori bacterium. BMC Chem. 13, 41 (2019). <https://doi.org/10.1186/s13065-019-0556-0>
53. E. D. Głowacki, M. Irimia-Vladu, S. Bauer, N.-S. Sariciftci, Hydrogen-bonds in molecular solids – from biological systems to organic electronics. J. Mater. Chem. B. 1, 3742–3753 (2013). <https://doi.org/10.1039/C3TB20193G>
54. K.-K. Mishra, K. Borish, G. Singh, P. Panwaria, S. Metya, M.-S. Madhusudhan, A. Das, Observation of an Unusually Large IR Red-Shift in an Unconventional S–H···S Hydrogen-Bond. J. Phys. Chem. Lett. 12, 1228–1235 (2021).
55. T.-M. Dhorajiwala, S.-T. Halder, L. Samant, Comparative In Silico Molecular Docking Analysis of L-Threonine-3-Dehydrogenase, a Protein Target Against African Trypanosomiasis Using Selected Phytochemicals. JABR. 6, 101–108 (2019). <https://doi.org/10.29252/JABR.06.03.04>
56. A.-P. Asmara, Kajian Integrasi Nilai-Nilai Karakter Islami Dengan Kimia Dalam Materi Kimia Karbon. JPS Unimus 4, 2 (2016).
57. J.-S. Gómez-Jeria, A. Robles-Navarro, G. Kpotin, N. Garrido-Sáez, G.-D. Nelson, Some remarks about the relationships between the common skeleton concept within the Klopman-Peradejordi-Gómez QSAR method and the weak molecule-site interactions. J. Chem. Res. 5, 32-52 (2020).